USGS
science for a changing world

Geological Field Trips in Southern Idaho, Eastern Oregon, and Northern Nevada

Edited by Kathleen M. Haller and Spencer H. Wood

Open-File Report 2004-1222

U.S. Department of the Interior
U.S. Geological Survey

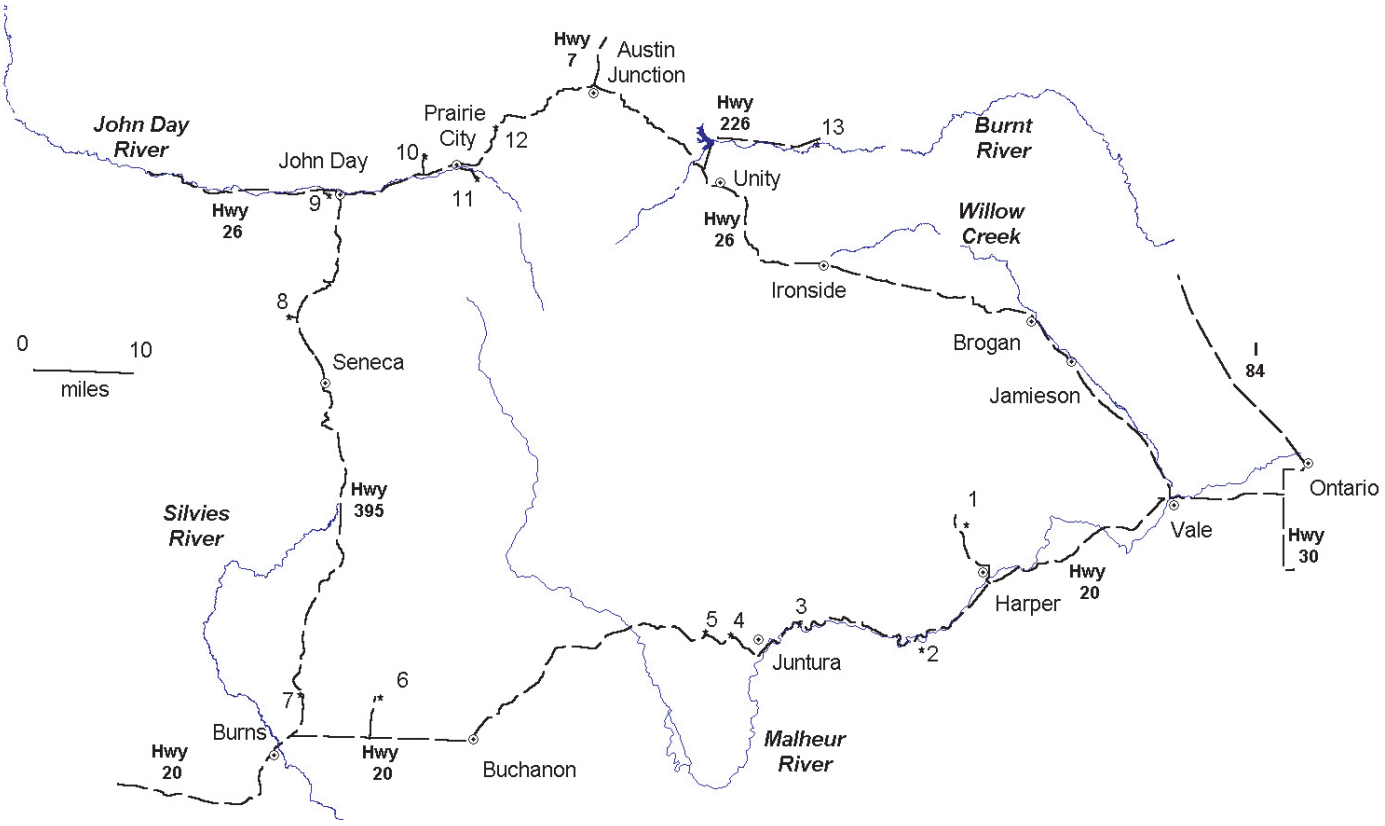

Figure 1. Sketch map of field-trip route. Trip begins at the intersection of Highway 26 and Highway 20, in the town of Vale, Oregon. We will overnight in Burns.

The Rattlesnake Tuff and Other Miocene Silicic Volcanism in Eastern Oregon

By Martin Streck[1] and Mark Ferns[2]

Regional Context of Miocene Silicic Volcanism

Two separate (well maybe not so separate) problems arise when we consider the middle Miocene rhyolite lava flows and ash-flow tuffs exposed along the field-trip route. First, what is the relationship between the older (~15.5 Ma) rhyolites (Dinner Creek Ash-flow Tuff and Littlefield Rhyolite) and the time correlative flood basalts of Columbia River Basalt Group to the north and Steens Basalt to the south? It now is clear that the Columbia River Basalt, the Steens Basalt, and the older rhyolites are part of a larger, bimodal magmatic province (Hooper and others, 2002). Plume-related and back-arc spreading models for the origin of the Columbia River Basalt must account for the very large volumes of silicic magmas that were generated in the southern half of this larger magmatic province. Additionally, genetic models must account for subsequent calc-alkaline volcanism, extension, and rapid subsidence along the Oregon-Idaho graben (Cummings and others, 2000).

Our second problem arises when we consider the younger (7–10 Ma) and equally extensive ash-flow tuffs that erupted from buried vents located to the west near Burns. How do they relate to the initial middle Miocene magmatism? The Burns area ash-flow tuffs (Devine Canyon, Prater Creek, and Rattlesnake ash-flow tuffs) are the largest ash-flow tuffs erupted from a westward-younging belt of rhyolite eruptive centers that culminates at Newberry Caldera (MacLeod and others, 1975). Oldest rhyolites in the west belt are Stockade Mountain and Duck Butte (10.4 Ma), located on the west flank of the Oregon-Idaho graben, just north of the Steens escarpment (MacLeod and others, 1975; Johnson and Grunder, 2000). The general westward-progression of rhyolitic magmatism is complicated by older, enigmatic, small rhyodacite domes near the town of Buchanan (~14 Ma, ~40 km east of Burns) and at Horsehead Mountain (15.5 Ma), west of Burns (MacLeod and others, 1975; MacLean, 1994). Small rhyolite and rhyodacite domes at Double Mountain (8.1 Ma) and ash flow tuffs at Kern Basin (12.6 Ma) record recurrent silicic eruptions on the east end of the trend, within the Oregon-Idaho graben proper (Ferns and others, 1993; Cummings and others, 2000).

The Rattlesnake Tuff

The 7.05-Ma Rattlesnake Tuff covers about 9,000 km^2 but reconstructed original coverage was between 30,000 and 40,000 km^2. Travel distances are among the farthest recorded (Wilson and others, 1995) and were in excess of 150 km from the inferred source near the center of the tuff's distribution based on existing outcrops. Eruption products are mostly (>99 percent) high-silica rhyolites that contain colored glass shards and pumice clasts with narrow and distinct ranges in major element composition but typically large ranges in incompatible trace elements (Streck and Grunder, 1997). Although volumetrically minor, a wide compositional spectrum is indicated by dacite pumices (<1 percent) and quenched basaltic inclusions (<<0.1 percent) that are almost exclusively found in dacite and dacite/rhyolite banded pumices (Streck and Grunder, 1999). Data are most consistent with the following petrogenetic scenarios in the evolution of the Rattlesnake Tuff magmatic system: (1) partial melting of mafic crust yielded rhyolitic melts that were compositionally close to observed, least-evolved high-silica rhyolites (Streck, 2002); (2) fractional crystallization dominated processes led to chemical gradients observed among five compositionally and mineralogically distinct rhyolitic magmas (Streck and Grunder, 1997); and (3) primitive tholeitic magmas stalled beneath rhyolites, evolved to enriched basaltic andesitic magmas (preserved in inclusions) and yielded dacitic compositions after mixing with least-evolved rhyolites (Streck and Grunder, 1999).

Thickness of tuff outcrops is remarkably uniform, ranging between 15 and 30 m for the most complete sections. Only 13 percent of the area is covered with tuff thicker than 30 m, to a maximum of approximately 70 m. Excellent preservation makes it possible to distinguish multiple welding and crystallization facies; in addition, rheomorphic tuff can be found within a radius of 40-60 km from the inferred source (Streck and Grunder, 1995).

[1]Department of Geology, Portland State University, Portland, OR 97207, streckm@pdx.edu

[2]Oregon Department of Geology and Mineral Industries, Portland OR 97207, mark.ferns@state.or.us

Based on vitric unaltered tuff, the entire welding range is subdivided into five mappable facies of welding that are (with associated bulk densities and porosities): nonwelded (<1.5 g/cm^3; >36 percent), incipiently welded (1.50-1.65 g/cm^3; 36-30 percent), partially welded with pumice (1.65-2.05 g/cm^3; 30-12 percent), partially welded with fiamme (2.05-2.30 g/cm^3; 12-2 percent), and densely welded (2.30-2.34 g/cm^3; <2 percent). In the partially welded zone, deformation of pumices precedes one of matrix shards and leads to fiamme composed of dense glass while the shard matrix has a remaining porosity of 12 percent or less.

Degree of welding generally decreases with distance from the source. Densely welded tuff is rare beyond approximately 70 km from the source, and partially welded tuff with fiamme is rare beyond approximately 130 km. A regional change in welding only is observed subtly in the highest welding degrees because strong local variations are often prevail. Local variations complicate simple welding scenarios that imply loss of temperature during travel and/or reduced tuff thickness with distance leads to less welding.

Strong local variations in welding are most dramatic near the source, where observed welding degrees encompasses the entire range. For example, at constant thickness (20±3 m) and over a distance of 1 to 3 km, nonrheomorphic outcrops can grade from an entirely nonwelded to incipiently welded vitric section to a mostly densely welded and crystallized section, where incipiently or less welded tuff is constrained to an approximately 1-m-thick basal zone and presumably a comparably thick top zone (now eroded). This is evident even though crystallization subsequent to welding reduces the vitric tuff proportion. Such strong local variations are interpreted to be the result of threshold-governed welding that imply combined parameters that control welding (T, P, P_{H2O}) create welding conditions that are significantly modified by slight variations in thickness and/or accumulation rate.

ROAD LOG

Mileage Inc.	Cum.	
0	0	Intersection of U.S. Highways 26 and 20 in Vale, Ore. (fig. 1).
2.6	2.6	Double Mountain (fig. 2), a rhyolite dome dated at about 8.1 Ma is visible to the southwest. Double Mountain is one of a number of small, late Miocene silicic centers erupted in

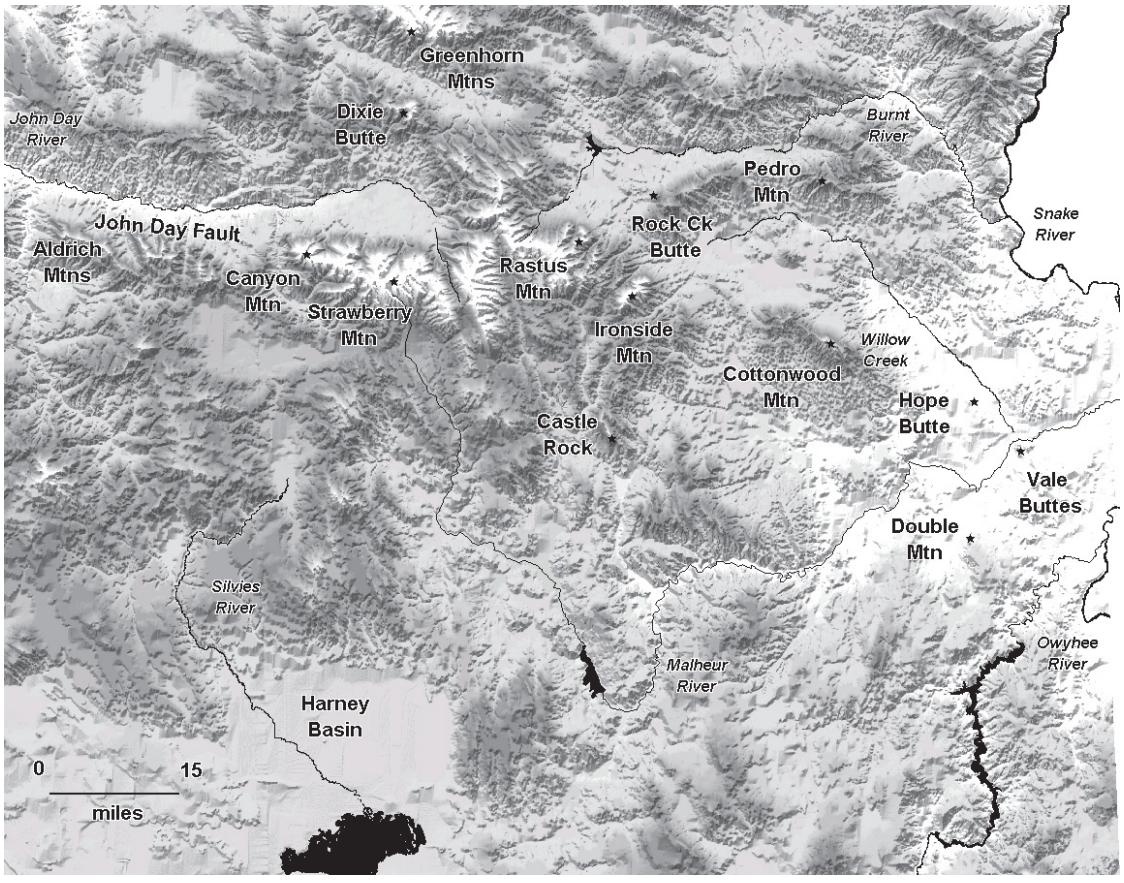

Figure 2. Main physiographic features along the field-trip route.

the central part of the Oregon–Idaho graben between 12 and 8 Ma (fig. 3).

4.0 6.6 Thick flow cropping out along the canyon walls of the Malheur River to the north is a late Miocene, hypersthene-bearing andesite. Referred to as the Vines Hill Andesite by Lees (1994), who reported an $^{40}Ar/^{39}Ar$ radiometric age of 10.25±0.94 Ma. Age is very similar to post Columbia River Basalt Group andesites near La Grande, which have yielded $^{40}Ar/^{39}Ar$ ages of 10.4 Ma (Ferns and others, 2002b).

4.5 11.1 Light-colored exposures are part of the Late Miocene–Pliocene Lake Idaho deposits.

1.2 12.3 Freshwater limestone is exposed overlying the Vines Hill andesite to the northwest. Note the exposures of cross-bedded gravels and sandstones along the highway east of the Vines Hill summit. The highway crosses several poorly expressed north-trending, down to the east faults between 12.3-13.2 mi that juxtapose gravel, limestone, and andesite.

0.9 13.2 Bar ditch exposures of fossiliferous freshwater limestone.

1.2 14.4 An older late Miocene sedimentary sequence is exposed beneath olivine basalt flows to the northwest. Rough radiometric ages from several olivine basalt flows indicate that they erupted at about 7.5 Ma.

0.7 15.1 Highway crosses through the very small town of Little Valley. Active hot springs come up along faults in this area.

2.8 17.9 Light-colored outcrops to the north and south are part of the Bully Creek Formation (Kittleman and others, 1965, 1967). The formation is made up of interbedded fine-grained tuffaceous sediments, diatomite, and interbedded ash-flow tuffs. These fine-grained sediments are unconformable across an older faulted sequence of interbedded arkosic sandstones, palagonitic tuffs, and calc-alkaline lava flows.

3.9 21.8 Turn to the right at Harper junction and cross the abandoned railroad line. TURN RIGHT and proceed to Harper, following the paved road.

0.4 22.3 TURN RIGHT and follow the paved road through Harper, which winds around and turns to the north.

5.6 27.9 If weather conditions allow, turn off of the paved road, proceed through the gate, and follow the dirt road to the cliff-forming outcrops to the north.

Stop 1. Tuff of Bully Creek

The ash-flow tuff prominently exposed here is the lower of two ash-flows mapped by Brooks and O'Brien, (1992a, 1992b) within the Bully Creek Formation. The upper ash-flow tuff, which is locally welded, displays the high Zr (1,200 ppm) signature that is characteristic for the Devine Canyon ash-flow tuff. The lower ash-flow tuff, named by Ferns and others (1993) as the tuff of Bully Creek, is a gray massive ash-rich, phenocryst-poor (<5 percent) tuff that at this location contains entrained and deformed clasts of diatomite and small pumices (~2 cm). Note the centimeter-wide subtle "lineations" across outcrop that are most likely gas-escape pipes. Also, note the fine-grained and glassy, thus excellently preserved, fall-out ash deposit at the base. We do not know whether this ash-flow tuff erupted from a nearby source or, like the Devine Canyon ash-flow tuff, is the distal deposit of a larger eruption, possibly near Burns(?). The ash-rich nature and small pumice size suggest the latter. Lees (1994) reports a $^{40}Ar/^{39}Ar$ age of 10.33±1.59 Ma from the olivine basalt flow that caps the ridge to the east. A question to consider here—Is there evidence in this outcrop for subaqueous flow into a shallow lake?

Mileage
Inc. Cum.

0.7 28.6 Return to the paved road and turn south, following the road back through Harper and onto Highway 20.

6.0 34.6 Turn right on Highway 20 and proceed west towards Burns.

3.0 37.6 Rounded yellow hills to the south are interbedded siltstones, sandstones, and palagonitic tuffs. Here Highway 20 crosses onto a bench formed by a resistant basalt sill. The basalt sill is more than 200-m thick and extends three-fourths of the way up the hill to the south. In places, the margins of the sill are marked by pepperite breccias, indicating intrusion into wet sediments.

1.5 39.1 Eroded hills to the north and south are erosional remnants of middle Miocene sediments. Radiometric ages from interbedded basalt and basaltic andesite flows record an extensive period of subsidence, sedimentation, and synvolcanic calc-alkaline volcanism starting at about 14.5 Ma. Synvolcanic hot spring activ-

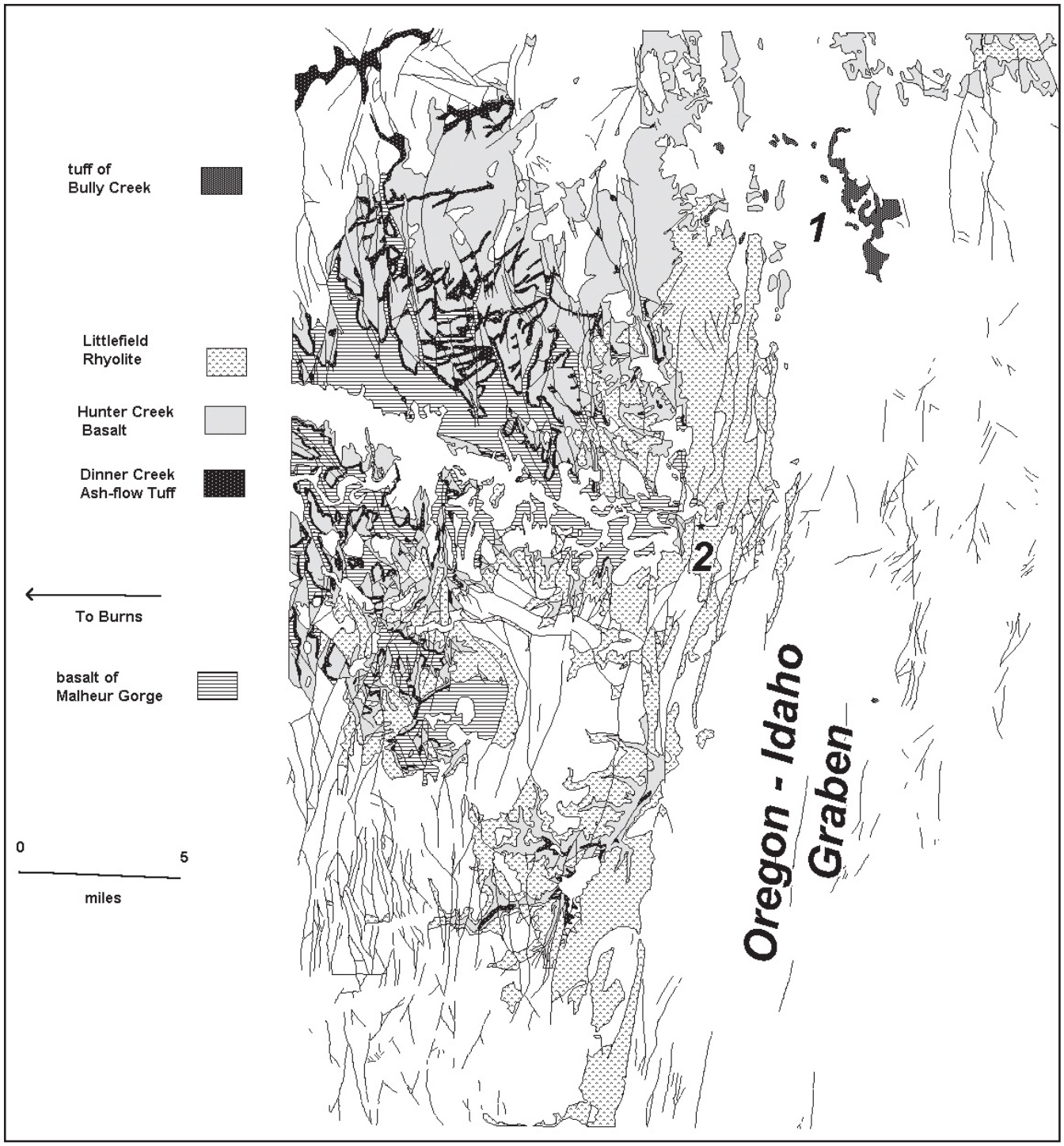

Figure 3. Geologic map of the lower Malheur River after Ferns and others (1993). Locations of Stops 1 and 2 are shown.

ity resulted in extensive areas of epithermal mineralization.

1.0 40.1 Red weathering exposures along the road to the south are part of the outcrops of Littlefield Rhyolite (Kittleman and others, 1965, 1967), which is made up of several very large rhyolite lava flows (fig. 3).

1.0 41.1 U.S. Highway 26 crosses one of the boundary faults to the Oregon-Idaho graben and enters into canyon lands cut by the Malheur River.

Exposures to the north and south are all large rhyolite lava flows.

2.0 43.1 TURN LEFT WITH CAUTION—BE ALERT FOR ONCOMING TRAFFIC onto old Highway 26, which follows along the south side of the Malheur River. We will follow the old highway to a point where all the vehicles can comfortably park; this is Stop 2.

Stop 2. Littlefield Rhyolite

Here the Malheur River cuts through silicic and mafic units that make up the Hog Creek sequence (Hooper and others, 2002). Thin ash-flow tuffs, including the Dinner Creek Ash-flow Tuff (Kittleman and others, 1965, 1967) and the tuff of Namorf (Ferns and O'Brien, 1992), and thick rhyolite lava flows, Littlefield Rhyolite (Kittleman and others, 1965, 1967), mark a transition from mafic to silicic volcanism. Base of the section here is marked by the Hunter Creek Basalt (Kittleman and others, 1967), a series of glassy, aphanitic mafic lava flows that are chemically and petrographically indistinguishable from flows of the Grande Ronde Basalt. The tuff of Namorf (Ferns and O'Brien, 1992), marked by yellow outcrops farther up the hill is perhaps the most inconspicuous ash-flow tuff in the Hog Creek sequence. This ash-rich, phenocryst-poor tuff here is partially welded and glassy. The ash-flow tuff underlies a vitrophyre flow breccia that locally marks the base of one of the large rhyolite lava flows that make up the Littlefield Rhyolite. We will take a closer look at very large basal flow lobes exposed in a side canyon.

The Littlefield Rhyolite is the westernmost example of the enigmatic, very large rhyolite lava flows that erupted during the middle Miocene in southeast Oregon and southwest Nevada. At least 3 separate flows are exposed in the cliff to the south forming a unit that extends over 850 km^2 representing about 100 km^3 of magma. Individual flows are typically glassy with small plagioclase and clinopyroxene phenocrysts. Individual flows can be traced over very large distances. Lees (1994) suggests that the glassy matrix is actually composed of super-welded glass shards, implying that the Littlefield Rhyolite is a series of rheomorphic ash-flow tuffs. Outcrop pattern suggests that the Littlefield Rhyolite may have erupted from linear vents along the western margin of the Oregon-Idaho graben.

Mileage
Inc. Cum.

0.4 43.5 PROCEED WITH CAUTION and turn left onto U.S. Highway 26, heading west toward Burns.

2.9 46.4 The basalt of Malheur Gorge (Evans, 1990; Hooper and others, 2002) is exposed on both sides of the river through here. For all intents and purposes, aphyric flows in the upper part of the basalt of Malheur Gorge cannot be distinguished from Grande Ronde Basalt.

5.5 51.9 Differential weathering of mappable units along the Malheur River has allowed geologists working here to clearly identify faults. The Dinner Creek Ash-flow Tuff is a prominent ledge former that can be easily identified at a distance. The Dinner Creek is nearly always overlain by the Hunter Creek Basalt, which characteristically weathers to form rounded hills mantled by fist-sized blocky talus. The overlying Littlefield Rhyolite typically forms prominent cliffs.

2.0 53.9 Hunter Creek Basalt to the left typically forms hackly-jointed exposures. Note the thin collonade beneath the thick, hackly jointed entabulature.

0.6 54.5 Evans (1990) notes that the Malheur River follows a northwest-trending graben structure. Erosional remnants of diatomaceous sediments and interbedded, partially welded ash-flow tuffs are exposed to the south. Geochemical analyses indicate that one of the ash-flow tuffs is the Devine Canyon Tuff.

0.6 55.1 Much more densely welded exposures of the older Dinner Creek Ash-flow Tuff form prominent cliff bands along the hills to the north and south of the river. Here the Dinner Creek serves as an excellent marker horizon that allows ready identification of faults.

9.3 64.4 Pull out to the right; this is Stop 3.

Stop 3. Dinner Creek Welded Ash-Flow Tuff

The Dinner Creek Welded Ash-flow Tuff (15.2 Ma; Hooper and others, 2002) is an important marker unit that separates the upper, rhyolite-dominated Hog Creek Formation from the basalt of Malheur Gorge. The Dinner Creek Tuff forms distinctive ledges that can be easily traced on both sides of the Malheur River. Mafic lava flows exposed below the Dinner Creek include a lower package of plagioclase phyric flows petrographically similar to the Steens Basalt and an upper package of aphanitic flows that, like the Hunter Creek Basalt, are petrographically and chemically similar to the Grande Ronde Basalt. The Dinner Creek Tuff is rhyolitic in composition and phenocryst poor. The tuff thickens toward a presumed vent area at or near Castle Rock (Rytuba and Vander Meulen, 1991). Based on distribution of mapped outcrops

correlated with the Dinner Creek, the ash-flow covered some 4,000 km^2.

The Dinner Creek Tuff is typically welded and marked by a basal vitrophyre. Devitrified zones are marked by irregular ovoid cavities and spherulites. This locality is somewhat atypical, as many of the cavities are filled with chalcedonic quartz. The tuff is about 20-m thick of which the lowest most 1–2 m consists of the non- to densely welded vitric base.

Mileage Inc.	Cum.	
3.3	67.7	Oasis Café in Juntura.
3.3	71.0	Turn right onto dirt road and drive about 0.1 mi up to the first rim (tilted); this is Stop 4.

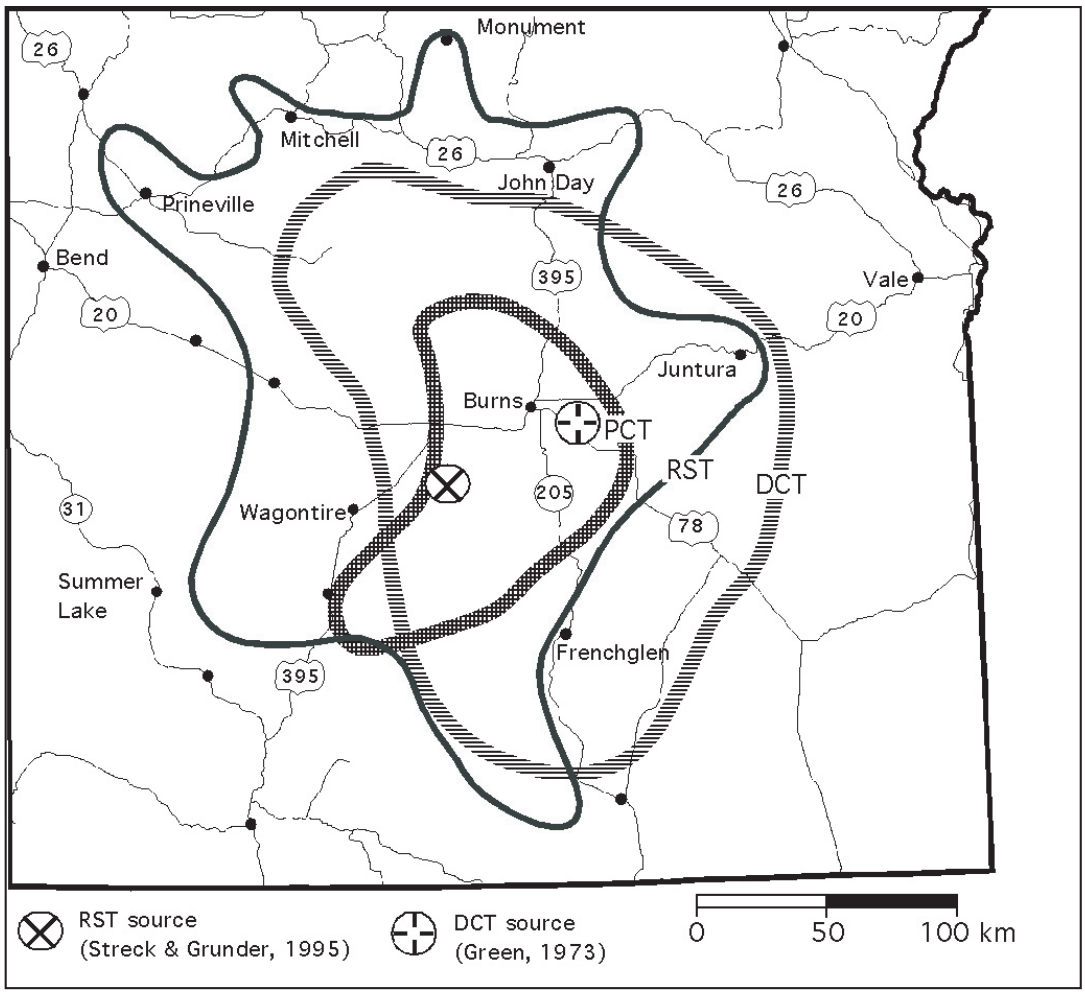

Figure 4. Inferred outlines and source areas of Harney Basin Tuffs. RST, Rattlesnake Tuff; PCT, Prater Creek Tuff; DCT, Devine Canyon Tuff. Outlines for DCT and PCT modified from Green (1973) and Walker (1979), respectively.

Stop 4. Devine Canyon Tuff

The Devine Canyon Tuff is crystal rich and originally covered more than 18,600 km^2 of southeastern Oregon, with a total volume of approximately 195 km^3 (Greene, 1973) (fig. 4). It is characterized by 10–30 percent phenocrysts of alkali feldspar and quartz, with sparse clinopyroxene. It varies from nonwelded to densely welded; most commonly it occurs as greenish-gray stony devitrified tuff. Thickness is about 30 m near the type section about 0.5 km northeast of the confluence with Poison Creek and corresponds to observed maximal thicknesses (Greene, 1973). $^{40}Ar/^{39}Ar$ age of 9.68±0.03 Ma was obtained from sanidine separates (Deino and Grunder, unpublished). At this location, the tuff is nearly densely welded, vitric and exhibits its crystal-rich nature. Tuff cliff is 4–5-m thick.

Mileage Inc.	Cum.	
8.9	79.9	OPTIONAL STOP (along road): diatomite and altered tuff with huge sanidines (~1 cm in diameter).
0.7	80.6	Park along road: Stop 5 is at Drinkwater Pass on descending side westward.

Stop 5. Diatomite and Devine Canyon Tuff

Here, Devine Canyon Tuff is non- to partially welded and vitric; it sits on top of diatomite. The tuff is excellently preserved and such fresh looking non-welded tuff of Devine Canyon Tuff is rather uncommon. Approximate thickness is 10 m.

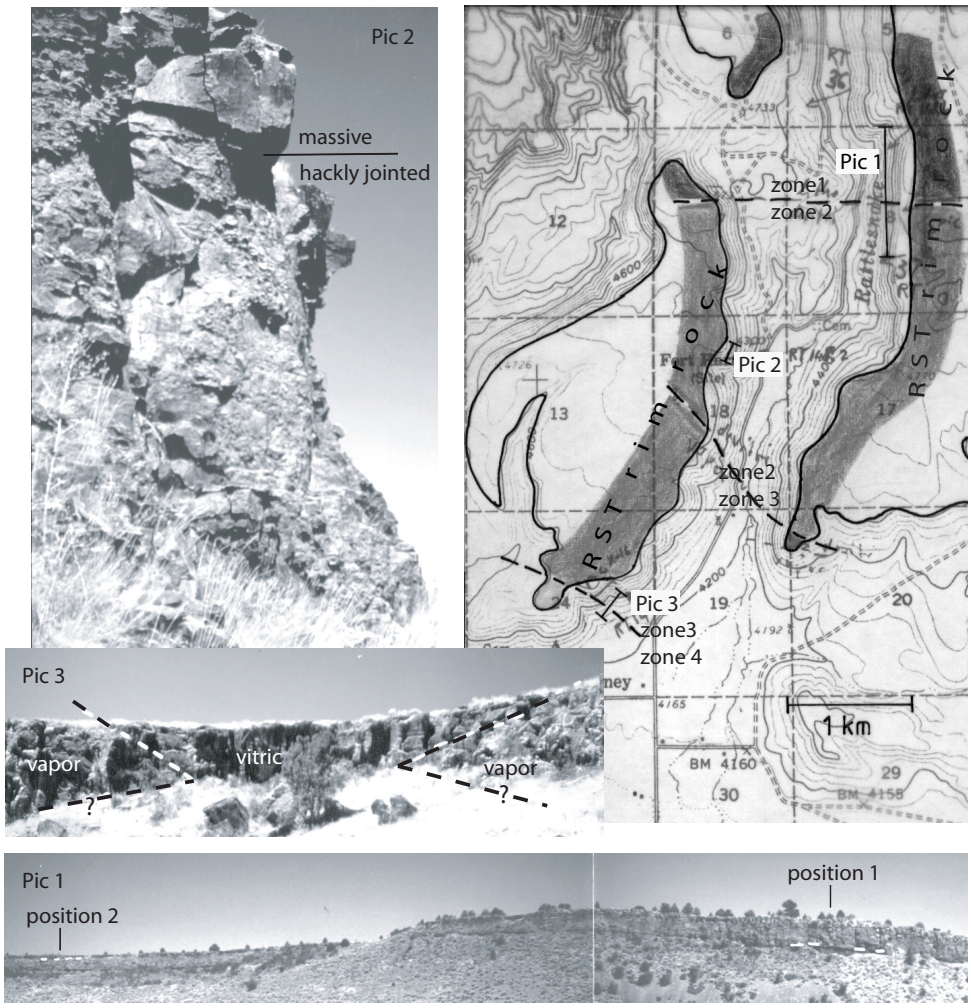

Figure 5. Overview of local facies changes. Zone 1: tuff dominated by thick lithophysal tuff underlying pervasively devitrified tuff and overlying (inferred, not exposed here) lower non- to densely welded vitric tuff. Zone 2: tuff dominated by pervasively devitrified tuff (Pic 2) overlying lower vitric tuff and underlying upper vitric tuff. Zone 3: tuff section consists of partially welded (with pumice) tuff that is vitric or vapor phase altered. Zone 4: vitric incipiently welded tuff. Picture 1: at position 1, densely welded vitrophyre exposed below white dashed line and section is topped with float of upper vitric tuff and at position 2, entire section below white dashed line is lithophysal tuff. Picture 2 shows pervasively devitrified tuff throughout in two facies, hackly jointed and massive. Picture 3: in middle of picture, tuff consists entirely of vitric tuff (vitric) that splits into a lower and upper vitric tuff separated by vapor phase tuff (vapor) further to the right and left, dashed lines indicate position of sharp interfaces between vitric and vapor phase tuff (analogous to the one seen in fig. 13 in Streck and Grunder, 1995).

Mileage Inc.	Cum.	
15.8	96.4	Stinkwater Pass.
0.3	96.7	Lithic-rich hydrovolcanic surge deposits.
5.4	102.1	Town of Buchanan.
3.0	105.1	Rims to right are Rattlesnake Tuff.
7.7	112.8	TURN RIGHT ON Rattlesnake Road.
4.9	117.7	PULL OUT to the right, this is part of Stop 6.

Stop 6. Strong Local Facies Changes in the Rattesnake Tuff

From the distance here and as we drive out of the canyon, we will observe how the Rattlesnake Tuff can drastically change in facies over a distance of 1–3 km without an apparent strong change in thickness (fig. 5). Local and strong facies changes are typical for the Rattlesnake Tuff (see above, Streck and Grunder, 1995) and complicate simple distance driven welding and alteration (high temperature) trends. Across from parking (Zone 2 and position 1 in fig. 5), Rattlesnake Tuff is 17-m thick and prominent outcrop cliff consists mostly of pervasively devitrified tuff underlain by 1.5 m densely welded vitric tuff (black vitrophyre) and capped by float of upper vitric, partially welded tuff. Just north of here (Zone 1, position 2 in fig. 5), outcrop is equally thick but most of section consists now of lithophysal tuff overlain by pervasively devitrified tuff—an analogue of this section with a more complete stratigraphy, but with similar proportional thicknesses of each zone, will be observed at Stop 7. As we drive back and out of Rattlesnake Creek, the first facies change is where thick middle pervasively devitrified section is lost (transition Zone 2-Zone 3 in fig. 5) and replaced by tuff that is partially welded with pumice and has a vapor phase altered zone as upper part (see fig. 13 in Streck and Grunder, 1995). And finally, this gives way to a incipiently welded, vitric tuff at mouth of canyon where the cliff is still 12-m high (Zone 4 in fig. 5).

Constraints on lower tuff boundaries at Stop 6 (*e.g.*, lower vitrophyre), flat lying tuff cliffs, and flat-topped rim rock topography indicate that facies changes are not associ-

ated with great topographic variations over the distance from Stop 6 to mouth of canyon. This suggests that tuff did not change thickness by more that a factor of about two. As mentioned above, Streck and Grunder (1995) interpreted this type of local facies change mostly as a function of the time span the tuff stayed hot above a critical welding temperature. Change in alteration facies is, in turn, largely a function of welding degree, temperature, and amount of vapor.

Mileage Inc.	Cum.	
5.8	123.5	Back on Highway 20.
9.8	133.3	TURN RIGHT at intersection with 395.
3.4	136.7	Pull out to the right, Stop 7.

Stop 7. Rattlesnake Tuff Type Section

This is the type locality of the Rattlesnake Ash-flow Tuff (Walker, 1979), herein referred to as Rattlesnake Tuff (RST). It is named for the original type locality on Rattlesnake Creek (John Day Valley), about 100 km north from here. Total thickness of the tuff at Stop 7 is 22 m. It is a highly zoned section and distance to inferred source is 51 km. The underlying pale-orange to buff-colored, fine-grained, poorly consolidated tuffaceous sedimentary sequence is a ubiquitous slope-forming unit throughout the Harney Basin.

The lowermost white 1-m-thick deposit likely is a precursory fallout deposit to the Rattlesnake Tuff (Streck and Grunder, 1997) resting on a soily substrate (fig. 6). It consists almost entirely of clear glass shards (note: later today we will observe tuff sections at Stops 9 and 11 that consist entirely of this type of glass shard matrix). The fallout deposit is conformably overlain by 0.5 m of nonwelded vitric RST with "mixed" shard matrix (clear and brown rhyolitic glass shards) and 7 to 10 percent white pumice up to 2 cm in diameter. In some places, the transition from the lower deposit to the nonwelded tuff is nearly gradational, and the transition may be overemphasized by the change from white to mixed shard matrix. Bubble wall shards can be seen in both nonwelded and layered deposit. The nonwelded zone grades abruptly to 0.5 m of partially welded vitric tuff, overlain by 1 m of black vitrophyre. The more than 19-m-thick capping cliff-forming unit is entirely lithophysal tuff. The lower 4 m of this section are divided into a perlitic black matrix base and upper part with spherulitic matrix. The upper 15 m are entirely lithophysae in a devitrified matrix and are capped by float of pevasively devirtrified tuff. Just across the highway (east) from this location, float on top of cliff-forming RST also includes upper vitric partially welded tuff indicating proximity to the inferred original top of the unit.

Continue from Stop 7 northward on 395. Highway 395 drives into Poison Creek canyon with excellent exposures of Harney Basin ignimbrite stratigraphy. Lowermost cliff is Devine Canyon Tuff (DCT) separated from the overlying Prater Creek Tuff (PCT) by poorly exposed tuff and tuffaceous sedimentary rocks. The sequence is capped by the Rattlesnake Tuff (RST). The bulk of the ignimbrites is composed of high-silica rhyolites that range from the slightly peralkaline DCT to the peralkaline/metaluminous RST and form important regional stratigraphic and structural markers.

Intercalated-tuffaceous sediments appear to thin until they are completely missing about 40–60 km from here, southward and northward. In the south, the Rattlesnake Tuff directly overlies the Devine Canyon Tuff that also is evident at Stop 8. Similarly, sediments thin westward suggesting

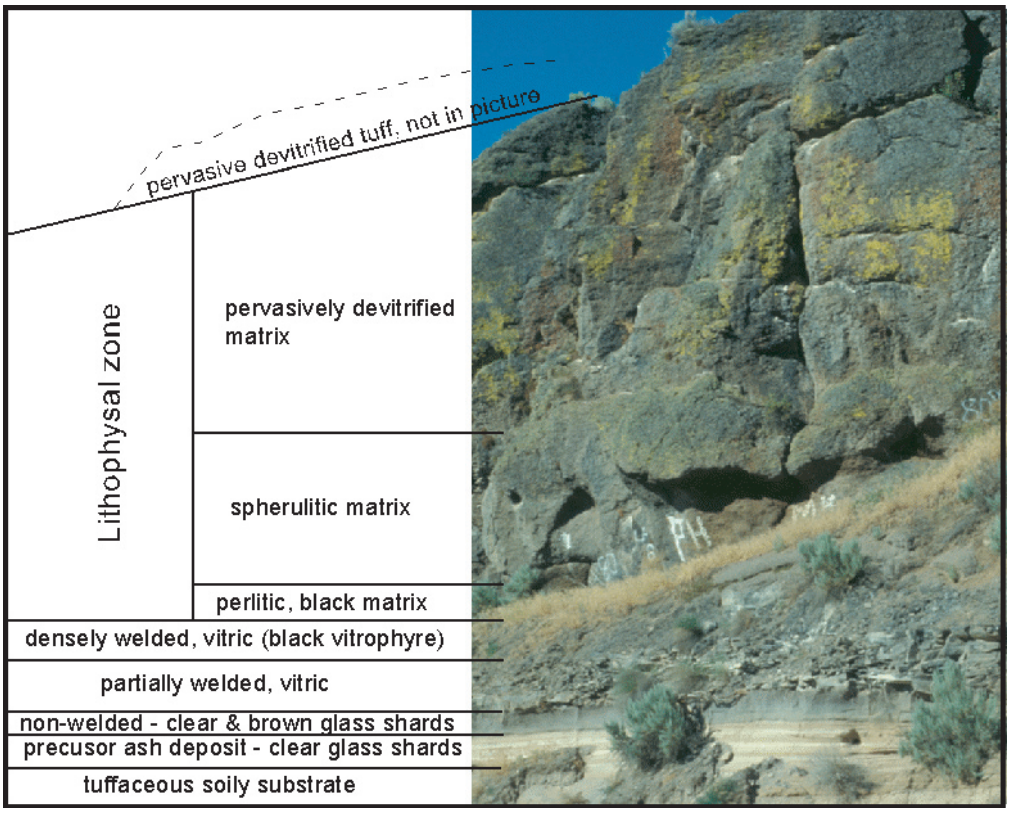

Figure 6. Outcrop stratigraphy of Rattlesnake Tuff at Stop 7.

an active basin existed between about 9 and 7 Ma around Burns extending into what is now the southern termination of the Blue Mountain uplift (Walker and Robinson, 1990).

The Prater Creek Tuff is mainly a devitrified, crystal-poor ash-flow tuff. Exposures of the type section (designated by Walker, 1979) can be seen from U.S. Highway 395 on the walls of Poison Creek where the maximum thickness is 12 m; lithologic variations can be seen in reference sections in Prater Creek, about 5 km east of Poison Creek. The type section consists chiefly of pale grayish-red, devitrified tuff with grayish-pink gas cavities up to about 2 cm in diameter. Flattened, devitrified-pumice fragments are present throughout but are not abundant. Alkali feldspar and quartz are sparse, and the tuff contains rare lithic fragments (Walker, 1979). Devitrified whole-rock tuff gave an age of 8.48±0.05 Ma (Deino and Grunder, unpublished).

Mileage Inc.	Cum.	
1.1	137.8	Prater Creek Tuff rim on left.
2.0	139.8	PULL OUT to the left for OPTIONAL STOP to view Harney Basin Tuff stratigraphy and to inspect partially welded Devine Canyon Tuff with pumices in size up to 30 cm.
10.8	150.6	Mermaid rhyolite flow.
5.5	156.1	Aldrich (left), Canyon (center), and Strawberry Mountains (right) in background (fig. 2). Topographic highs are related to the eroded volcanic edifices of the Strawberry volcanics and to the upthrown side of a high-angle fault. It is thought to be a fairly young reverse fault that substantially displaces the 7.05 Ma Rattlesnake Tuff. The fault trends east-west along the John Day Valley.
18.9	175	Town of Seneca.
7.4	182.4	TURN LEFT at intersection with Izee-Paulina road.
0.3	182.5	Gravel pit in Devine Canyon Tuff, entrance on south side of Izee-Paulina road.
0.8	183.3	Park on either side and walk up dirt road to the north towards open forest. Small cliff outcrop about 30 m past the fence. Small outcrop is Stop 8.

Small cliff outcrop is vitric non- to incipiently welded Rattlesnake Tuff. Tuff also is pumiceous, even though the distance to inferred source is 98 km and thus, the tuff has lost its biggest pumices (average maximum pumice size is 12.3 cm; near the source it reaches >50 cm). Tuff is mostly vitric and displays variously colored glass shards from dark brown to white (clear under microscope) (see fig. 2 in Streck and Grunder, 1997). All shard populations are high-silica rhyolite and coincide lithologically and chemically with high-silica pumice populations (Streck and Grunder, 1997). This mixed-shard matrix observed here is the northernmost exposure of this overall dark, "salt and pepper" appearance. From here northward, the glass matrix consists also of mixed shards, however, darker populations are lost leading to a lighter appearance in outcrop. Similar light tuff is observed closer to the vent only as basal parts of tuff sections, as was observed in basalt part of section at Stop 7.

Before driving back to intersection with U.S. Highway 395, note low subdued hills to the west. These are the erosional tuff remnants of mostly Devine Canyon Tuff as observed at Stop 6. Thus, younger Rattlesnake overlie the older Devine Canyon at this location.

On the way back to U.S. Highway 395, optional Stop at gravel pit exposing vitric, partially welded Devine Canyon Tuff similar to what we observed at Stops 4 and 5. Distance to Stop 5 is about 100 km (figs. 1, 2, and 4).

Mileage Inc.	Cum.	
4.1	187.4	Canyon Mountain ahead (ophiolite complex) As you drive towards John Day—you pass by outcrops of serpentinite after the main decline into the valley when road is on river level.
14.2	201.6	Intersection of U.S. Highway 395 with U.S. Highway 26 in John Day (side trip to Stop 9 from intersection 395 and 26).
1.1	202.7	Intersection of Highway 26 and 47B-Turn left on 47B.
0.5	203.2	Intersection 47B and 47—Turn left on 47.
1.2	204.4	Rattlesnake Tuff outcrop on left: Stop 9.

Stop 9. Thick Distal Rattlesnake Tuff

At Stop 9 we can see an approximately 22-m-thick section of Rattlesnake Tuff in contact with underlying substrate material, a conglomerate consisting of a variety of lithologies eroded from the Aldrich, Canyon, and Strawberry Mountains (side note: the Canyon Mountain ophiolitic complex was exposed at the time since its lithologies can be found as pebbles and cobbles in the conglomerate). This location is 118 km from the inferred RST source. Lithological zonations at Stop 9 include a 1-m-thick nonwelded zone, overlain by about 8 m of partially welded tuff (lower part, about half, "with pumice" and upper half "with fiamme" thus exhibiting higher welding, fig. 7). Lower vitric tuff is overlain by pervasively devitrified tuff (6–8-m thick) and capped by a 2-m-thick vapor phase zone (*i.e.*, porous devitrified tuff). This section illustrates that

only the degree of welding of the thickest tuff sections are systematic indicators of distance-dependent decrease in welding. The highest welding degree of this deposit is "partially welded with fiamme" and not densely, although tuff sections with similar thickness exhibit densely welded zones if closer to the source. No black vitrophyre (*i.e.*, dense welding) was observed beyond a distance of about 70 km. Therefore, an overall temperature decrease and/or volatile loss with distance is indicated very subtly. Another feature to observe here, in comparison to Stop 8, is that this section consists of a matrix characterized by shards that mostly represent the most evolved rhyolite compositions, thus it lacks dark brown coloration.

Mileage Inc.	Cum.	
2.8	207.2	Back at intersection of U.S. Highways 26 and 395 in John Day, continue east on U.S. Highway 26 towards Prairie City.
5.0	213.2	On north side of road, exposures are mainly mafic lavas and one tuff near the base, which will be observed at Stop 10. The tuff likely is the Mascall ignimbrite. For discussion later at Stop 10, note stratigraphic sequence.
0.9	214.1	Lowest most cliffs are more outcrops of Mascall ignimbrite.
1.4	215.5	Crossing John Day River, lower rims on the left (north), about 10-m-thick Mascall ignimbrite.
1.1	216.6	TURN Left (north) on country road, side trip to Stop 10.
1.9	218.5	Mascall outcrop (cliff) on E side a few meters up the slope is Stop 10.

Stop 10. Lithic Rich Tuff—Mascall Ignimbrite

Exposed is a lithic and pumice-rich partially welded vitric tuff. The tuff is correlative based on lithological characteristics with the Mascall ignimbrite of Davenport (1971) found in the Paulina Basin 80 km west southwest from here. The ignimbrite was named for its occurrence near the base of the Mascall formation. The Mascall formation was established by Merriam (1901) for a sedimentary sequence near the Mascall Ranch and in the vicinity of Picture Gorge, proper. The tuff was dated by K-Ar yielding an age of 15.8±1.4 Ma that is consistent with mammalian fossils of Barstovian age found above the ignimbrite (Davenport, 1971). Mineral phases in the Mascall ignimbrite are anorthoclase, magnetite, green clinopyroxene, and zircon, and bulk composition is high-silica rhyolite with 75 weight percent SiO_2 (Davenport, 1971). The Mascall ignimbrite is characterized by abundant (5–10 percent) lithic obsidian clasts, which distinguish this tuff from the Rattlesnake Tuff that is otherwise lithologically similar. Widespread occurrence of abundant obsidian clasts may suggest that pyroclastic eruptions leading to the Mascall ignimbrite reworked previous dome material that predated the voluminous Mascall eruption. Chemical analysis to evaluate this hypothesis is currently underway. Although Mascall ignimbrite outcrops occur sparsely, their spacing of about 100 km apart indicate that the Mascall ignimbrite also was an originally widespread tuff unit resulting from a voluminous, likely-caldera forming eruption. Petrography and composition indicate affinities to Harney Basin tuffs and thus an original source for the Mascall ignimbrite may lie well to the south.

The correlation of this outcrop and outcrops nearby (see above and below) with the Mascall ignimbrite has significant stratigraphic implications. The thick section of mafic lava flows, which has been visible in the bluffs north of U.S. Highway 26 east of John Day, cannot be

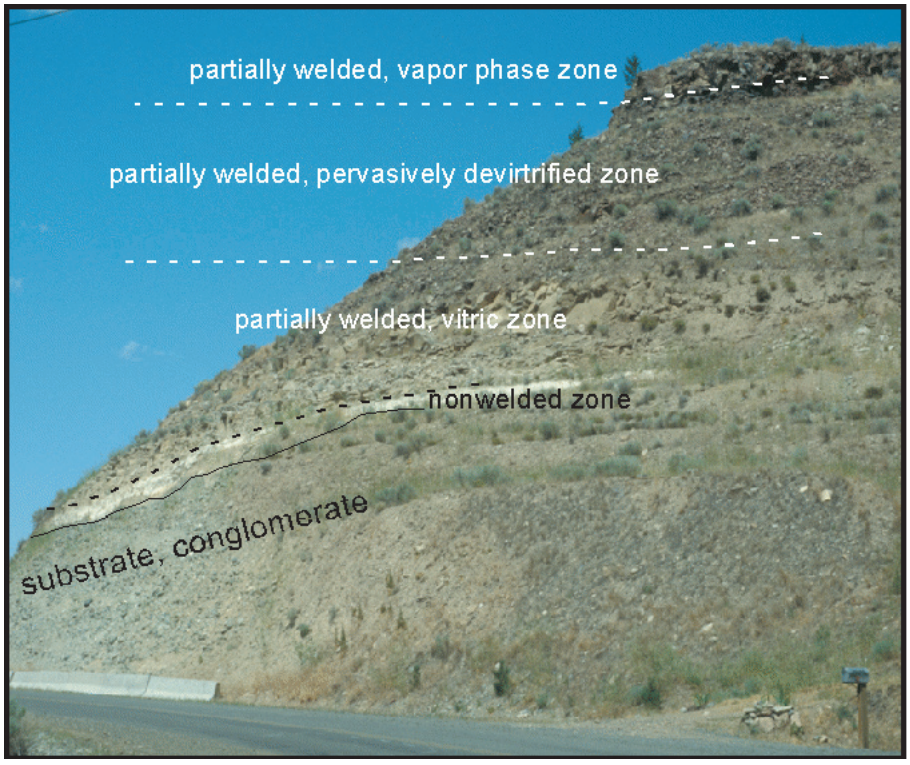

Figure 7. Outcrop stratigraphy of Rattlesnake Tuff at Stop 9.

Picture Gorge Basalt flows because of their post-Mascall age (Mascall formation overlies unconformably the Picture Gorge basalts at Picture Gorge). Much of the area north and west from here was previously mapped as Columbia River Basalt (Thayer and Brown, 1964; Brooks and others, 1984). However, chemical analyses may imply that this area is underlain mainly by younger calc-alkaline flows (see analyses in Brooks and others, 1984) that more properly belong in the Strawberry Volcanics of Thayer and Brown (1964). Very limited geochemical analyses from mafic lavas flows north of here in apparently the same stratigraphic position as the post-Mascall flows present here, do not correlate with chemistries of any of the Picture Gorge flows.

RETURN TO U.S. Highway 26 and continue east towards Prairie City.

Mileage Inc.	Cum.	
2.5	221	U.S. Highway 26 cuts into Mascall ignimbrite, which also is exposed as cliff on north side of road.
3.0	224	Intersection Main Street and U.S. Highway 26 in Prairie City: Side trip to Stop 11 from this intersection; TURN RIGHT onto Main Street and continue.
0.4	224.4	TURN Left into Bridge Street at intersection of Main Street and Bridge Street; continue on Bridge Street that will turn into country road #62 after next intersection; Stop 11 (along country road #62).
4.2	228.6	Park in turn out next to outcrop on south side of road. Light outcrops are Stop 11.

Stop 11. Non-Welded Rattlesnake Tuff

Outcrop is 4-m thick and consists entirely of nonwelded Rattlesnake Tuff. Distance to inferred source is 133 km and thus pumices are small. Average maximum size is 4 cm. This outcrop is extraordinary for the nonwelded nature, yet excellent preservation. Outcrop is entirely glassy and shards are mostly clear and, if juxtaposed with matrix of Stop 8, a strong color contrast is apparent that reflects the change in proportions among shard populations. Material from this outcrop was used for welding experiments of Grunder and Druitt and Quane and Russell (both submitted to JVGR's special volume on welding).

TRACK BACK TO intersection Main Street and U.S. Highway 26 in Prairie City, continue on U.S. Highway 26 eastward.

Mileage Inc.	Cum.	
6.4	235.0	Stacked sequence of olivine basalt flows and underlying lithic ash-flow tuff is exposed in the hills immediately to the north of U.S. Highway 26. Although the olivine basalt flows generally are considered to be part of the Picture Gorge Basalt, not enough work has been done on them to confirm that correlation. Presence of an underlying ash-flow tuff here is troubling.
0.2	235.2–235.5	**OPTIONAL STOP.** Oligocene(?) ignimbrite. Directly along east side of road, small outcrops of biotite and amphibole bearing welded tuff. Presence of biotite and amphibole in the tuff here suggests that it may be an Oligocene ash-flow tuff. Oligocene–early Miocene tuffs elsewhere in the region, at Tower Mountain and near Unity Reservoir (Ferns and others, 2001), generally contain hydrous mineral phases, in contrast to the middle Miocene ash-flow tuffs, which generally do not. Radiometric dates are needed before this conundrum can be resolved. The overlying olivine basalt flows appear more similar to the early calc-alkaline mafic eruptions associated with the Powder River Volcanic Field (Ferns and others, 2001; 2002a) than to the Picture Gorge Basalt. The olivine basalt flows may represent early stages of Strawberry Volcanics magmatism.
4.4	239.9	TURN OUT on right shoulder for Stop 12.

Stop 12. Early Oligocene Dacite at the Fireside Inn—33 Ma

Here we will look at one of the older Oligocene bimodal volcanic centers exposed in northeast Oregon. Early Oligocene silicic eruptions produced distinctive, coarse-textured porphyritic dacites and rhyolites that, unlike most of the later middle Miocene ash-flow tuffs, contain hydrous mineral phases such as biotite and hornblende. The road cut exposes a dacite dome and dome breccia that is cut by several porphyritic basalt dikes. Although this particular dome has not been dated, nearby porphyritic dacites have yielded radiometric ages of about 33.6 Ma (Ferns and others, 1982) and 33.7 Ma (Urbanczyk, 1990). Similarly aged granodiorite intrusions to the southeast (Hooper and others, 1995) and possibly to the west are associated with porphyry copper mineralization. Somewhat younger (~25–28 Ma) eruptions of rhyolitic ash-flow tuffs accompanied formation of large calderas at Tower Mountain (Ferns and others, 2001).

Mileage Inc.	Cum.	
2.1	242.0	Some of the oldest (~42 Ma) Tertiary volcanic rocks exposed in northeast Oregon form columnar jointed outcrops on the north side of U.S. Highway 26, just east of the Dixie Mountain pass. Andesite breccias of similar age are exposed on the side of Dixie Mountain to the north, filling an eroded surface of older pre-Tertiary rocks. Pre-Tertiary rocks exposed along U.S. Highway 26 to the east are parts of a serpentinite-matrix mélange.
0.9	244.1	Prominent outcrops of basaltic andesite exposed along the road here are part of the Slide Creek Basalt (Robyn, 1979) the basal member of the Strawberry Volcanics. Age of the Slide Creek generally is considered to be about 15 Ma.
4.0	248.1	Continue east on U.S. Highway 26, through Austin Junction, bypassing the turn off to Baker City and Sumpter. The Greenhorn Mountains, which form the high ridge to the northwest, are part of a serpentinite-matrix mélange.
0.7	248.8	Diatomite and tuffaceous sediments are exposed beneath a basalt flow. Although generally considered to be part of the Slide Creek Basalt, this flow may be younger than the Slide Creek. The diatomite beds locally contain abundant leaf fossils and may be similar in age to Bully Creek Formation.

Strawberry Volcanics

The Strawberry Volcanics, originally defined by Thayer (1957) is one of the largest, most diverse, and most poorly mapped units in eastern Oregon. Although generally considered to be middle Miocene in age and representative of a post-Columbia River Basalt Group calc-alkaline complex (Robyn, 1979), areas now mapped as Strawberry Volcanics contain both older late Oligocene–early Miocene rhyolite and dacites (Walker and Robinson, 1990) and younger late Miocene–Pliocene mafic lavas. Much of the area was heavily forested when first mapped. Subsequent large forest fires have considerably reduced the amount of concealing ground cover, making this region an ideal candidate for future mapping and study.

Mileage Inc.	Cum.	
4.2	253.0	Red-weathering basaltic andesite flow with abundant, large plagioclase phenocrysts. Not clear where this flow lies in respect to the diatomite section.
2.8	255.8	Platy andesite flow.
3.7	259.5	Tuffaceous sediments are exposed beneath andesite flows as U.S. Highway 26 descends into the upper end of the Burnt River valley.
1.8	261.3	Aphyric basalt flow; overlies tuffaceous sediments and, to the south, ash-flow tuff.
2.1	263.4	Badlands topography with erosional remnants of basalt flows overlying tuffaceous sediments. Thick ash flow is exposed in ditch beneath basalt flow to south.
1.5	264.9	Intersection of Highway 245 and U.S. Highway 26. Side trip to Stop 13 (optional). Proceed left onto Highway 245 and continue 2.6 miles to Unity Reservoir. Note: Cumulative mileage does not include this side trip.

Stop 13. Unity Reservoir

Ridge to north of reservoir is a fault block capped by what appears to be an older Oligocene ash-flow tuff. According to Reef (1983), there are three ignimbrite units exposed in the upper part of the fault block (fig. 8)—a lower pumiceous tuff, an overlying, densely welded vitric tuff; and a capping, partially welded lithic tuff. All three seem to be associated with basal vitrophyres. The lower two tuffs contain biotite crystals. A thick rhyolite dome truncates the ash-flow tuffs to the northwest. The ash-flow tuff rests atop a series of thick rhyodacite lahars and tuff breccias. A rhyodacite clast in the tuff breccia has a K/Ar age of 19.5 Ma (Fiebelkorn and others, 1983). Fossilized palm boles have been found in the top of an ash-flow further to the east.

Mileage Inc.	Cum.	
0.1	265.0	An uplifted block of pre-Tertiary basement rocks is exposed to the south. West flank of the uplift is unconformably overlain by flows of the Strawberry Volcanics. The uplift, the exposed front of which forms Bullrun Rock and Rastus Mountain, is cored by mineralized Oligocene porphyry intrusions (Hooper and others, 1995).
3.1	268.1	Town of Unity—The Waterhole and the High Country Café.
1.8	269.9	Rock Creek Butte, at 12:30, is a slab of peridotite in another uplifted block of basement

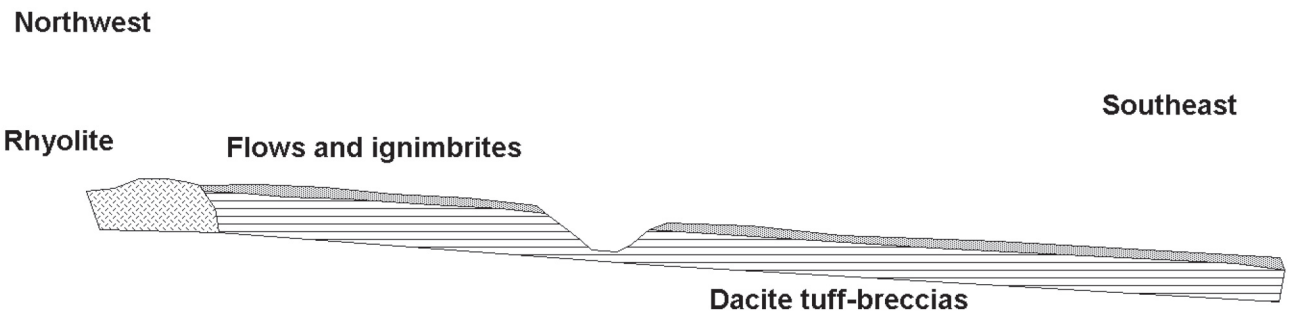

Figure 8. Stratigraphic section at Stop 13 at Unity Reservoir.

rock. Rock Creek Butte marks a pre-Tertiary terrane boundary.

4.8	274.7	Columnar jointed porphyritic lava flow, not known whether it is Miocene or older in age.
1.3	276.0	The thick ash-flow tuff exposed along the road here is mapped as Dinner Creek Tuff. Note that exposures here are much thicker than those seen along the Malheur River.
0.9	276.9	The prominent butte to the south is Ironside Mountain. Formed by dacite and rhyolite flows filling a small, oval depression above Jurassic sediments. Although considered to be a complex folded fault structure (Thayer and Brown, 1973) it might be a collapsed central vent structure related to the eruption of middle Miocene ash flows.
0.2	277.1	Jurassic volcaniclastic sediments of the Weatherby Formation (Brooks, 1979) exposed along the highway.
0.5	277.6	Highway crosses onto younger Pliocene lava flows first mapped by Brooks and others (1976). Flows are alkalic lavas and part of the Keeney Creek.
1.2	278.8	Eldorado Pass. Late Miocene to Pliocene, fluvial and lacustrine sediments are exposed that underlie the Keeney Creek Formation.
6.9	285.7	Rounded hill to east is a Pliocene cinder cone that still retains a cone form.
0.6	286.3	Town of Ironside, high ground in distance is Pedro Mountain, a late Jurassic–early Cretaceous intrusion. Intrusion was emplaced along a pre-Tertiary terrane boundary. Pedro Mountain is cut by a swarm of north-trending Columbia River Basalt dikes. Geochemical analyses indicate the dikes are all Grande Ronde Basalt. Black double butte in the middle ground is another one of the small Keeney Creek vents.
6.9	293.2	High ridge to the south is Cottonwood Mountain, which is made up of pre-Tertiary rocks, Malheur Gorge Basalt flows, and capping Littlefield Rhyolite flows. Hooper and others (2002) consider the upper basalt of Malheur Gorge to be correlative with the Grande Ronde Basalt. Small hill to the left is Cow Valley Butte, a small, undated, granitic intrusion assumed to be of late Jurassic–early Cretaceous age.
4.0	297.2	At Cow Creek, more basalt of Malheur Gorge flows exposed to right.
6.2	303.4	Underlying exposures of Jurassic sediments, Weatherby Formation (Brooks, 1979).
1.4	304.8	Pliocene Keeney Creek Formation flows to east.
2.3	307.1	A large displacement fault runs along the foot of Cottonwood Mountain to the southwest; in places it cuts alluvial fans. This may well be an active Holocene fault.
2.1	309.2	Town of Brogan.
2.4	311.6	Low hills are eroded remnants of late Miocene and Pliocene sediments. Sediments can be traced eastward into the western Snake River Plain. Generally considered that they were deposited in the large Pliocene Lake Idaho.
3.7	315.3	Town of Jamieson.
0.8	316.1	Rounded butte to the right at 2:30 is Hope Butte. Top of the butte is underlain by hot spring sinter deposits. Hot spring activity was accompanied by mercury and gold mineralization.

0.9	317	Vale Buttes comes into view at 11:30. The buttes are a hydrothermally hardened mass of Pliocene sandstone and siltstone. Several active hot springs vent into the river from the west side of the buttes. Alteration zones are marked by mercury and gold mineralization.
15.5	332.5	Intersection of U.S. Highways 26 and 20.

END of road log

References

Brooks, H.C., 1979, Geologic map of the Huntington and part of the Olds Ferry quadrangles, Baker and Malheur Counties, Oregon: Oregon Department of Geology and Mineral Industries Geologic Map Series GMS-13, scale 1:62,500.

Brooks, H.C., McIntyre, J.R., and Walker, G.W., 1976, Geology of the Oregon part of the Baker 1 degree x 2 degree quadrangle: Oregon Department of Geology and Mineral Industries Geological Map Series GMS-7, scale 1:250,000.

Brooks, H.C., Ferns, M.L., and Avery, D.G., 1984, Geology and gold deposits of the southwest quarter of the Bates quadrangle, Grant County, Oregon: Oregon Department of Geology and Mineral Industries Geological Map Series GMS-35, scale 1:24,000.

Brooks, H.C., and O'Brien, J.P., 1992a, Geology and mineral resources map of the Westfall quadrangle, Malheur County, Oregon: Oregon Department of Geology and Mineral Industries Geologic Map Series GMS-71, scale 1:24,000.

Brooks, H.C., and O'Brien, J.P., 1992b, Geology and mineral Resources map of the Little Valley quadrangle, Malheur County, Oregon: Oregon Department of Geology and Mineral Industries Geologic Map Series GMS-72, scale 1:24,000.

Cummings, M.L., Evans, J.G., Ferns, M.L., and Lees, K.R., 2000, Stratigraphic and structural evolution of the middle Miocene syn-volcanic Oregon-Idaho graben: Geological Society of America Bulletin, v. 112, p. 668–682.

Davenport, R.E., 1971, Geology of the Rattlesnake and older ignimbrites in the Paulina basin and adjacent area, central Oregon: Corvallis, Oregon State University, unpublished Ph.D. thesis, 132 p.

Evans, J.G., 1990, Geology and mineral resources map of the Jonesboro quadrangle, Malheur County, Oregon: Oregon Department of Geology and Mineral Industries Geological Map Series GMS-66, scale 1:24,000.

Ferns, M.L., Brooks, H.C., and Ducette, J., 1982, Geology and mineral resources map of the Mt Ireland quadrangle, Baker and Grant Counties, Oregon: Oregon Department of Geology and Mineral Industries Geologic Map Series GMS-22, scale 1:24,000.

Ferns, M.L., and O'Brien, J.P., 1992, Geology and mineral resources map of the Namorf quadrangle, Malheur County, Oregon: Oregon Department of Geology and Mineral Industries Geologic Map Series GMS-74, scale 1:24,000.

Ferns, M.L., Brooks, H.C., Evans, J.G., and Cummings, M.L., 1993, Geologic map of the Vale 30' x 60' quadrangle, Malheur County, Oregon and Owyhee County, Idaho: Oregon Department of Geology and Mineral Industries Geologic Map Series GMS-77, scale 1:100,000.

Ferns, M.L., Madin, I.P., and Taubeneck, W.H., 2001, Reconnaissance geologic map of the La Grande 30' x 60' quadrangle, Baker, Grant, Umatilla, and Union Counties, Oregon: Oregon Department of Geology and Mineral Industries Reconnaissance Map Series RMS-1, scale 1:100,000.

Ferns, M.L., McConnell, V.S., and Madin, I.P., 2002a, Geology of the surface and subsurface of the southern Grande Ronde Valley and lower Catherine Creek drainage, Union County, Oregon: Oregon Department of Geology and Mineral Industries Open File Report O-02-02.

Ferns, M.L., McConnell, V.S., and Van Tassell, J., 2002b, Geology of the Imbler quadrangle, Union County, Oregon: Oregon Department of Geology and Mineral Industries Geology Map Series GMS-114, scale 1:24,000.

Fiebelkorn, R.B., Walker, G.W., MacLeod, N.S., McKee, E.H., and Smith, J.G., 1983, Index to K-Ar determinations for the State of Oregon: Isochron/West, v. 37, p. 3–60.

Greene, R.C., 1973, Petrology of the welded tuff of Devine Canyon, southeastern Oregon: U.S. Geological Survey Professional Paper 792, 26 p.

Hooper, P.R., Housemann, M.D., Beane, J.E., Caffrey, G.M., Enght, K.R., Scrivner, J.V., and Watkinson, A.J., 1995, Geology of the northern part of the Ironside Mountain inliern, northeastern Oregon, *in* Vallier, T.L., and Brooks, H.C., eds., Petrology and tectonic evolution of pre-Tertiary rocks of the Blue Mountains region: U.S. Geological Survey Professional Paper 1438, p. 415–457.

Hooper, P.R., Binger, G.B., and Lees, K.R., 2002, Ages of the Steens and Columbia River flood basalts and their relationship to extension-related calc-alkalic volcanism in eastern Oregon: Geological Society of America Bulletin, v. 114, p. 43–50.

Johnson, J. A., and Grunder, A.L., 2000, The making of intermediate composition magma in a bimodal suite—Duck Butte eruptive center, Oregon, USA: Journal of Volcanology and Geothermal Research, v. 95, p. 175–195.

Kittleman, L.R., Green, A.R., Haddock, G.H., Hagood, A.R., Johnson, A.M., McMurray, J.M., Russell, R.G., and Weeden, D.A., 1965, Cenozoic stratigraphy of the Owyhee region, south-eastern Oregon: University of Oregon Museum of Natural History Bulletin, 45 p.

Kittleman, L.R., Green, A.R., Haddock, G.H., Hagood, A.R., Johnson, A.M., McMurray, J.M., Russell, R.G., and Weeden, D.A., 1967, Geologic map of the Owyhee region, Malheur County, Oregon: University of Oregon Museum of Natural History Bulletin, scale 1:125,000.

Lees, K.R., 1994, Magmatic and tectonic changes through time in the Neogene volcanic rocks of the Vale area, Oregon, northwestern U.S.A.: Milton Keynes, U.K., Open University, unpublished Ph.D. thesis, 283 p.

MacLean, J.W., 1994, Geology and geochemistry of Juniper Ridge, Horsehead Mountain and Burns Butte—Implications for the petrogenesis of silicic magmas on the High Lava Plains, southeastern Oregon: Corvallis, Oregon State University, unpublished M.S. thesis, 141 p.

MacLeod, N.S., Walker, G.W., and McKee, E.H., 1975, Geothermal significance of eastward increase in age of Upper Cenozoic rhyolitic domes in southeastern Oregon: U.S. Geological Survey Open-File Report 75-348, 21 p.

Merriam, J.C., 1901, A contribution to the geology of the John Day Basin: University of California Publications in Geological Sciences 2, p. 269–314.

Robyn, T.L., 1979, Miocene volcanism in eastern Oregon—An example of calc-alkaline volcanism unrelated to subduction: Journal of Volcanological and Geothermal Research, v. 5, p. 149–161.

Reef, J.W., 1983, The Unity Reservoir rhyodacite tuff-breccia and associated volcanic rocks, Baker County, Oregon: Pullman, Washington State University, unpublished M.S. thesis, 128 p.

Rytuba, J.J., and Vander Meulen, D.B., 1991, Hot-spring precious-metal systems in the Lake Owyhee volcanic field, Oregon-Idaho, *in* Raines, G.L., Lisle, R.E., Schafer, R.W., and Wilkinson, W.H., eds., Geology and ore deposits of the Great Basin: Reno, Geological Society of Nevada, Symposium Proceedings, April 1–5, 1990, v. 2, p. 1085–1096.

Streck, M.J., 2002, Partial melting to produce high-silica rhyolites of a young bimodal suite—Compositional constraints among rhyolites, basalts, and metamorphic xenoliths: International Journal of Earth Sciences, v. 91, p. 583–593.

Streck, M.J., and Grunder, A.L., 1995, Crystallization and welding variations in a widespread ignimbrite sheet—The Rattlesnake Tuff, eastern Oregon: Bulletin of Volcanology, v. 57, p. 151–169.

Streck, M.J., and Grunder, A.L., 1997, Compositional gradients and gaps in high-silica rhyolites of the Rattlesnake Tuff, Oregon: Journal of Petrology, v. 38, p. 133–163.

Streck, M.J., and Grunder, A.L., 1999, Enrichment of basalt and mixing of dacite in the rootzone of a large rhyolite chamber—Inclusions and pumices from the Rattlesnake Tuff, Oregon: Contributions to Mineralogy and Petrology, v. 136, p. 193–212.

Thayer, T.P., 1957, Some relations of later Tertiary volcanology and structure in eastern Oregon: International Geological Congress, Volcanologia del Cenozoico, v. 1, p. 231–245.

Thayer, T.P. and Brown, C.E., 1964, Pre-Tertiary orogenic and plutonic intrusive activity in central and northeastern Oregon: Geological Society of America Bulletin, v. 75, p. 1255–1261.

Thayer, T.P. and Brown, C.E., 1973, Ironside Mountain, Oregon—A Late Tertiary volcanic and structural enigma: Geological Society of America Bulletin, v. 84, p. 489–497.

Urbanczyk, K.M., 1990, Geology of the eastern part of the Clarno Formation, northeast Oregon: Pullman, Washington State University, unpublished Ph.D. thesis, 263 p.

Walker, G.W., 1979, Revisions to the Cenozoic stratigraphy of Harney Basin, Oregon: U.S. Geological Survey Bulletin 1475, 35 p.

Walker, G.W., Robinson, P.T., 1990, Cenozoic tectonism and volcanism of the Blue Mountains region, *in* Walker G.W., ed., Geology of the Blue Mountains region of Oregon, Idaho, and Washington: U.S. Geological Survey Professional Paper 1437, p. 119–135.

Wilson, C.J.N., Houghton, B.F., Kamp, P.J.J., and McWilliams, M.O., 1995, An exceptionally widespread ignimbrite with implications for pyroclastic flow emplacement: Nature, v. 378, p. 605–607.